Article

Not peer-reviewed version

A Digital Twin of Empagliflozin Pharmacokinetics and Pharmacodynamics

Jennesse Alejandro , Michelle Elias , Mariia Babaeva , Matthias König *

Posted Date: 20 March 2026

doi: 10.20944/preprints202603.1559.v1

Keywords: digital twin; empagliflozin; Type 2 diabetes mellitus; physiologically based pharmacokinetic/pharmacodynamic model (PBPK/PD); pharmacokinetics; pharmacodynamics; personalized medicine

 doi:10.20944/preprints202603.1559.v1

Article

A Digital Twin of Empagliflozin Pharmacokinetics and Pharmacodynamics

Jennesse Alejandro[1], Michelle Elias [2], Mariia Babaeva [3] and Matthias König [2,4]*

[1] Brown University, Division of Biology and Medicine, 185 Meeting Street, Providence, RI 02912, USA
[2] Humboldt-Universität zu Berlin, Faculty of Life Sciences, Department of Biology, Institute of Theoretical Biology, Systems Medicine of the Liver, Unter den Linden 6, 10099 Berlin, Germany
[3] Charité – Universitätsmedizin Berlin, Charité Medical Faculty, Charité Campus Mitte, Charitéplatz 1, 10117 Berlin, Germany;
[4] University of Stuttgart, Institute of Structural Mechanics and Dynamics in Aerospace Engineering, Pfaffenwaldring 27, 70569 Stuttgart, Germany
* Correspondence: koenigmx@hu-berlin.de (M.K.)

Abstract

Background/Objectives: Empagliflozin is an SGLT2 inhibitor prescribed for the management of type 2 diabetes mellitus, lowering blood glucose by increasing urinary glucose excretion (UGE) through inhibition of renal glucose reabsorption. PK/PD responses vary substantially across patient populations, complicating dose selection under altered organ function. Here, we developed a whole-body PBPK/PD digital twin integrating absorption, distribution, metabolism, and excretion with explicit modeling of renal glucose handling via the renal threshold for glucose. **Methods:** The model represents empagliflozin and its glucuronide metabolite, is implemented in SBML, and was calibrated and evaluated against curated PK/PD data from 27 clinical studies spanning healthy individuals, patients with type 2 diabetes, and cohorts with renal or hepatic impairment. **Results:** The model accurately captured observed clinical PK/PD data across all 27 studies, spanning a wide range of doses, dosing regimens, and patient populations. Good agreement between simulations and observations was obtained under normal and impaired renal and hepatic function, as well as under fasted and fed conditions, demonstrating the model's ability to reproduce empagliflozin disposition and pharmacodynamic response across clinically relevant scenarios. **Conclusions:** This SBML-based PBPK/PD digital twin provides quantitative insight into empagliflozin dose dependency and the impact of renal impairment, hepatic impairment, and food intake on PK/PD across clinically relevant populations. All model files, simulation scripts, and curated datasets are openly available in accordance with FAIR principles.

Keywords: digital twin; empagliflozin; Type 2 diabetes mellitus; physiologically based pharmacokinetic/pharmacodynamic model (PBPK/PD); pharmacokinetics; pharmacodynamics; personalized medicine

1. Introduction

Type 2 diabetes mellitus (T2DM) is a chronic metabolic disorder and a major global health challenge, characterized by persistent hyperglycemia that can lead to severe complications. Despite the availability of multiple glucose-lowering therapies, many patients fail to achieve sustained glycemic control [1,2], highlighting the continued need for effective and well-characterized therapeutic strategies.

The kidney plays a central role in glucose homeostasis by reabsorbing nearly all filtered glucose in the proximal tubule [3], a process mediated primarily by sodium–glucose co-transporter 2 (SGLT2, ∼90%) and to a lesser extent by sodium–glucose co-transporter 1 (SGLT1, ∼10%) [4,5]. SGLT2 inhibition lowers the renal threshold for glucose (RTG), thereby increasing urinary glucose excretion (UGE) and reducing plasma glucose concentrations via an insulin-independent mechanism [5,6].

 doi:10.20944/preprints202603.1559.v1

Empagliflozin is an orally active SGLT2 inhibitor approved for the treatment of adults with T2DM. It is administered once daily, with a default starting dose of 10 mg that may be escalated to 25 mg for improved glycemic control in appropriate patients. Dosing is primarily guided by indication, renal function, and tolerability [7].

The pharmacokinetics of empagliflozin are well characterized. Following oral administration, it is rapidly absorbed with an oral bioavailability of ∼70–80% and peak plasma concentrations reached within 1.3–3 h. Plasma profiles show a biphasic decline with a terminal half-life of approximately 10–13 h, supporting once-daily dosing [8,9]. Food is considered to have no clinically relevant effect on absorption [10,11]. Empagliflozin has a large apparent volume of distribution and high plasma protein binding (∼86–90%, primarily to albumin). Metabolism is dominated by phase II glucuronidation via UGT2B7, UGT1A3, UGT1A8, and UGT1A9, forming 2-O-, 3-O-, and 6-O-glucuronide metabolites, each representing less than 10% of total drug-related material; oxidative metabolism is minimal [7,12]. Elimination occurs via both renal and fecal routes, with approximately 10–20% of the dose excreted unchanged in urine at steady state. Renal impairment increases exposure, while hepatic impairment has less than a 2-fold effect, and dose adjustment for liver disease is generally considered not required [12]. Pharmacodynamically, empagliflozin potently and selectively inhibits SGLT2 in the proximal tubule, lowering the RTG and producing dose-dependent increases in UGE, with sustained reductions in plasma glucose and HbA1c independent of insulin secretion [12].

Patients with T2DM exhibit substantial inter-individual variability in empagliflozin pharmacokinetics (PK) and pharmacodynamics (PD), with renal and hepatic function representing key sources of this variability. As eGFR declines, renal clearance of empagliflozin decreases, leading to modest increases in systemic exposure, while C_{max} remains largely unchanged. Despite higher exposure, UGE falls steeply with worsening renal function because less glucose is filtered, substantially attenuating the glycemic PD effect [13,14]. Hepatic impairment, by contrast, has comparatively minor effects on empagliflozin exposure and does not materially alter UGE or glucose-lowering efficacy, since the PD effect is driven by renal filtration rather than hepatic function. Routine dose adjustment is therefore not required in mild–moderate hepatic impairment, though caution is advised in severe disease due to limited data [15]. Together, these pathophysiological factors introduce a level of complexity in dose selection that mechanistic modeling approaches are well suited to address, enabling systematic assessment of drug exposure and response across diverse patient populations.

Several computational models of empagliflozin have been published, spanning population PK and PK/PD analyses [16–20], mechanistic and exposure–response PK/PD models [21–23], PBPK approaches [24–26], a quantitative systems pharmacology model of renal glucose handling [27], and a molecular binding study [28]. While these models have provided valuable insights into empagliflozin exposure–response relationships and glycemic effects, most rely on closed software and proprietary datasets, provide no executable code, and do not adhere to FAIR principles, precluding independent reproduction, long-term preservation, and systematic extension. Many are furthermore based on narrowly defined patient cohorts, limiting their applicability across the full range of clinically relevant populations and scenarios. A systematic overview of existing models, including their scope, availability, and reproducibility, is provided in Supplementary Table S1.

Reproducibility remains a broad challenge in systems biology [29] and PBPK modeling [30], with many published models lacking accessible equations, data, or executable workflows. Physiologically based pharmacokinetic/pharmacodynamic (PBPK/PD) modeling provides a quantitative framework for integrating physiological, biochemical, and drug-specific data, and by representing absorption, distribution, metabolism, and excretion (ADME) in mechanistic detail, such models can simulate the impact of organ dysfunction and other patient-specific factors on drug exposure and response, offering insights that complement and extend those obtainable from clinical trials alone [31–33]. To fully realize this potential, however, models must be transparent, reproducible, and built on openly accessible data and code.

 doi:10.20944/preprints202603.1559.v1

Here, we present a fully reproducible digital twin of empagliflozin developed in accordance with FAIR principles [34] and Open Science practices, using published clinical data from 27 studies (Table 1), including healthy individuals, patients with T2DM, and individuals with renal or hepatic impairment. The model is a physiologically based whole-body PBPK/PD framework that explicitly represents empagliflozin and its glucuronide metabolite (EG), as well as the key organs involved in absorption, metabolism, and elimination (intestine, liver, and kidney) linked through the systemic circulation and renal glucose handling. All clinical data are stored in a curated database, and the model is implemented in SBML [35] as a standardized format to ensure transparent and reproducible simulations. The digital twin was calibrated and evaluated across multiple datasets and applied to systematically investigate the effects of dose, renal impairment, hepatic impairment, and food intake on empagliflozin pharmacokinetics and pharmacodynamics. The digital twin quantitatively links parent drug and metabolite to pharmacodynamic response under normal and impaired organ function, providing a mechanistic, physiology-based framework that can be individualized to simulate patient-specific drug response across clinically relevant scenarios.

2. Materials and Methods

The digital twin of empagliflozin was developed through a systematic workflow combining clinical data curation, mechanistic PBPK/PD modeling, and *in silico* simulation. This involved a structured literature search, implementation of an SBML-based model, parameter optimization against a selected data subset, and simulation experiments designed to reflect clinical trial conditions. Pharmacokinetic and pharmacodynamic outcomes were analyzed to characterize empagliflozin disposition and variability across physiological, pathophysiological, and prandial states.

2.1. Systematic Literature Research and Data Curation

A systematic literature search was conducted to identify studies reporting pharmacokinetic and/or pharmacodynamic data for empagliflozin. PubMed was queried on 2024-08-27 using the terms "empagliflozin AND pharmacokinetics", and the PKPDAI database was screened in parallel [36]. Eligible studies included healthy volunteers, patients with type 2 diabetes mellitus, and populations with renal or hepatic impairment; animal studies and reports lacking sufficient data were excluded. An overview of the selection process is provided in Supplementary Figure S1.

Data from eligible studies were curated in the open pharmacokinetics database PK-DB [37], following established extraction protocols. Extracted information included demographics, disease status, dosing regimens, plasma and urine concentration–time profiles of empagliflozin and EG, and pharmacodynamic outcomes including UGE. Figure-based data were digitized using WebPlotDigitizer [38], and tabular or textual data were reformatted into standardized PK-DB formats. The complete curated dataset is publicly available via PK-DB and within the model files; an overview of included studies is provided in Table 1.

2.2. Computational Model

The PBPK/PD model was developed in the Systems Biology Markup Language (SBML) [35, 39]. Programmatic model construction and visualization were performed using the sbmlutils [40] and cy3sbml [41,42] libraries. Numerical solutions of the underlying ordinary differential equations (ODEs) were obtained with sbmlsim [43], powered by the high-performance SBML simulation engine libRoadRunner [44,45]. The complete model, including simulation scripts and documentation, is available in SBML format under a CC-BY 4.0 license via GitHub (https://github.com/matthiaskoenig/empagliflozin-model) and archived on Zenodo (v0.5.4) [46].

The model comprises a whole–body framework with submodels for the intestine, liver, and kidney, linked through the systemic circulation (Figure 1) to characterize empagliflozin absorption, distribution, metabolism, and excretion. The model has a hierarchical structure, with the whole–body model linking the individual organ submodels.

 doi:10.20944/preprints202603.1559.v1

Key ADME processes include intestinal absorption, hepatic glucuronidation via UGT enzymes to form the empagliflozin glucuronide metabolites (EG), and biliary excretion of EG with subsequent enterohepatic circulation. The kidney submodel captures both renal glucuronidation of empagliflozin to EG and urinary excretion of empagliflozin and EG. The pharmacodynamic component links empagliflozin plasma concentrations to UGE through inhibition of renal glucose reabsorption in the proximal tubule, parameterized by fasting plasma glucose and the RTG. Mathematical descriptions of the submodels and the corresponding ordinary differential equations are provided in the Supplementary Materials Section S4.

Fractional organ volumes and blood flows were taken from literature sources [31]. The fractional compartment volumes were set to $FV_{gu} = 1.71\,\%$ for the gut, $FV_{ki} = 0.44\,\%$ for the kidneys, $FV_{li} = 2.10\,\%$ for the liver, and $FV_{lu} = 0.76\,\%$ for the lungs. Fractional blood flows were defined as $FQ_{gu} = 18.00\,\%$ for the gut, $FQ_{ki} = 19.00\,\%$ for the kidneys, $FQ_{h} = 21.50\,\%$ for the hepatic venous outflow, and $FQ_{lu} = 100\,\%$ for the lungs. Absolute organ volumes and blood flows were calculated by scaling the corresponding fractional values with bodyweight.

Several key factors influencing pharmacokinetic and pharmacodynamic variability were implemented as scaling parameters:

- **Renal impairment** was modeled as a progressive decline in renal function using the scaling factor f_{renal}, applied to glomerular filtration rate (GFR) and renal clearance of empagliflozin and EG. Scaling values were derived from KDIGO categories: normal (eGFR $\geq$90 mL/min, $f_{renal\ function} = 1.00$), mild (eGFR 60–89 mL/min, $f_{renal\ function} = 0.69$), moderate (eGFR 30–59 mL/min, $f_{renal\ function} = 0.32$), and severe (eGFR <30 mL/min, $f_{renal\ function} = 0.19$), consistent with KDIGO guidelines and related modeling studies [47,48].
- **Hepatic impairment** was modeled using the scaling factor $f_{cirrhosis}$, representing reduced functional liver parenchyma and portosystemic blood shunting. Values were assigned according to Child–Turcotte–Pugh (CTP) classes: A (mild, 5–6 points, $f_{cirrhosis} = 0.40$), B (moderate, 7–9 points, $f_{cirrhosis} = 0.70$), and C (severe, 10–15 points, $f_{cirrhosis} = 0.81$) [49–52].
- **Food intake** was modeled using the absorption scaling factor $f_{absorption}$, which modulates the rate of intestinal empagliflozin absorption. Fasting and not-reported conditions were assigned $f_{absorption} = 1.00$, while fed conditions were assigned $f_{absorption} = 0.80$, consistent with the modest reduction in absorption rate observed after food intake.

Subject- and study-specific physiological and clinical parameters were incorporated where available, including bodyweight, glomerular filtration rate to adjust renal function, and fasting plasma glucose for the pharmacodynamic component. Multiple-dose regimens were implemented by stepwise numerical integration between dosing intervals, with dosing events applied according to study-specific protocols. Oral doses were specified using the parameter $PODOSE_{emp}$. Simulation time horizons and post-dose sampling windows were selected to match the corresponding clinical study designs.

2.3. Model Assumptions

Additional details on model equations and assumptions are provided in Supplementary Material S4. The key model assumptions and simplifications are summarized below.

- Empagliflozin absorption was modeled as a first-order process.
- Diurnal variation in plasma glucose concentrations was not modeled explicitly. Instead, a constant fasting plasma glucose concentration was assumed and used for the calculation of UGE. When reported, study-specific FPG values were used; otherwise, default values of 5.0 mM for healthy subjects and 8.0 mM for subjects with T2DM were assumed.
- The RTG was parameterized via parameter optimization, with optimized values reported in Supplementary Table S5.
- Renal filtration and tubular glucose reabsorption were not modeled explicitly. Instead, renal elimination of empagliflozin and EG was described using first-order processes dependent on

 doi:10.20944/preprints202603.1559.v1

kidney volume, renal function, and compound-specific excretion rate constants. The parameters KI_EMPEX_k and KI_EGEX_k were estimated via parameter optimization.

- The glucuronidation of empagliflozin to EG in the liver and kidneys was modeled using irreversible Michaelis–Menten kinetics, with UGT activity represented by the general scaling factor f_{ugt}.

2.4. Model Parameterization

A subset of curated data from healthy subjects, patients with T2DM, and individuals with renal impairment following single-dose administration was used for parameter optimization using a local standard optimizer. The resulting optimal parameter set was applied consistently across all subsequent simulations without further study-specific refitting. Optimized parameter values and optimization diagnostics are reported in Supplementary Materials Section S5, including fitted pharmacokinetic and pharmacodynamic parameter sets as well as convergence behavior and goodness-of-fit assessments for both model components.

Parameter optimization minimized a cost function $F(\vec{p})$ defined as the sum of squared weighted residuals $r_{i,k}$ across all time courses k and data points i:

$$F(\vec{p}) = 0.5 \sum_{i,k} (w_{i,k} \cdot r_{i,k}(\vec{p}))^2,$$

where weights $w_{i,k} = n_k/\sigma_{i,k}$ combine weighting by study sample size n_k and inverse measurement uncertainty $\sigma_{i,k}$, such that data points with lower uncertainty and larger sample sizes contribute more to the objective function.

Optimization was performed sequentially: pharmacokinetic parameters were estimated first, followed by pharmacodynamic parameters. To improve robustness against local minima, multiple optimization runs ($n = 100$) were conducted using different initial parameter values.

2.5. Simulations

For each curated clinical study (Table 1), a corresponding *in silico* experiment was implemented to reproduce the reported dosing regimen and study conditions. Study-specific parameters, including oral dose, prandial state, bodyweight, fasting plasma glucose, and renal or hepatic function were adjusted according to available study information, with multiple dosing protocols incorporated where applicable.

To systematically investigate sources of variability, parameter scans were conducted across physiologically relevant ranges of dose, renal function, hepatic function, and food intake, enabling a comprehensive evaluation of their influence on empagliflozin PK/PD outcomes.

2.6. Pharmacokinetic and Pharmacodynamic Parameters

Pharmacokinetic parameters of empagliflozin and its metabolites were calculated from plasma concentration-time curves and urinary excretion using standard non-compartmental methods. Pharmacodynamic outcomes were evaluated in terms of UGE, calculated from the simulated plasma concentration-time courses in combination with fasting plasma glucose and the renal threshold for glucose. Simulated profiles and derived pharmacokinetic and pharmacodynamic parameters were compared against the curated clinical data.

3. Results

3.1. Empagliflozin Database

An extensive database of empagliflozin pharmacokinetic and pharmacodynamic data was compiled to develop and evaluate the model. A systematic literature search across PubMed, PKPDAI, and manual sources initially yielded 191 records after duplicate removal. After screening according to predefined inclusion and exclusion criteria, 27 studies were selected for detailed curation and

 doi:10.20944/preprints202603.1559.v1

formed the core dataset used to develop and evaluate the PBPK/PD model. The complete study selection process is outlined in Supplementary Materials Figure S1. All curated pharmacokinetic and pharmacodynamic data are publicly available in the model files and in the PK-DB database, with unique study identifiers as referenced in the manuscript (Table 1).

3.2. Computational Model

Using the curated dataset, a digital twin in the form of a PBPK/PD model was developed to describe the ADME of empagliflozin and EG, as well as the pharmacodynamic effect on UGE (Figure 1). The complete model, including simulation scripts and documentation, is available in SBML format under a CC-BY 4.0 license via GitHub (https://github.com/matthiaskoenig/empagliflozin-model) and archived on Zenodo (v0.5.4) [46].

Simulations followed the respective clinical study designs, accounting for single- and multiple-dose regimens, as well as renal and hepatic impairment conditions. Dose and glucose dependency simulations are provided in Supplementary Materials Section S6.1 (Figures S7–S8), and individual study simulations in Section S6.2 (Figures S9–S38). The final optimized parameter set is summarized in Supplementary Materials Table S5. Parameter convergence and goodness-of-fit metrics are shown in Supplementary Materials Figures S5–S6. Submodel visualizations are provided in Supplementary Materials Section S3 (Figures S2–S4), and all model equations and ODEs are given in Section S4.

3.3. Dose Dependency

The pharmacokinetic and pharmacodynamic effects of empagliflozin over an oral dose range of 0–800 mg are shown in Figure 2. With increasing doses, plasma concentrations of empagliflozin and EG increased proportionally, as did the cumulative amounts excreted in urine and feces. The parameter scan showed a clear dose-dependent rise in exposure metrics ($AUC_{0-\mathrm{inf}}$ and C_{max}), while T_{max} and half-life remained largely unchanged across the dose range. Higher doses were associated with a nonlinear increase in UGE. Time-course simulations were performed for all curated clinical dose-dependency studies (Heise2013 [8], Heise2013a [53], Macha2015a [54], Sarashina2013 [55], Seman2013 [56], Zhao2015 [57]). Simulated empagliflozin plasma concentrations and UGE are shown for both single- and multiple-dose regimens, with model predictions in good agreement with the observed clinical data across all studies and dose levels.

3.4. Renal Impairment

The impact of renal impairment on empagliflozin disposition and pharmacodynamics is shown in Figure 3. Simulations were performed across a continuous range of renal function, with discrete categories corresponding to normal, mild, moderate, and severe impairment. With declining renal function, plasma concentrations of empagliflozin increased modestly, while EG plasma exposure rose more markedly. Urinary excretion of both empagliflozin and EG decreased progressively with worsening impairment, whereas EG fecal excretion increased compensatorily. Parent $AUC_{0-\mathrm{inf}}$ showed a moderate increase with declining renal function, while C_{max} and T_{max} were less affected. Renal clearance of empagliflozin decreased in parallel with the decline in GFR.

The pharmacodynamic response showed a pronounced reduction in UGE with declining renal function. In severe renal impairment, simulated UGE was markedly lower than under normal renal function, consistent with the attenuated glycemic efficacy observed clinically at low eGFR.

Simulated empagliflozin and EG plasma time courses, urinary excretion profiles, and UGE across renal function groups are shown together with clinical data from two studies (Macha2014f [13] and Sarashina2014 [14]). The model predictions align closely with the observed clinical data across all renal function categories.

 doi:10.20944/preprints202603.1559.v1

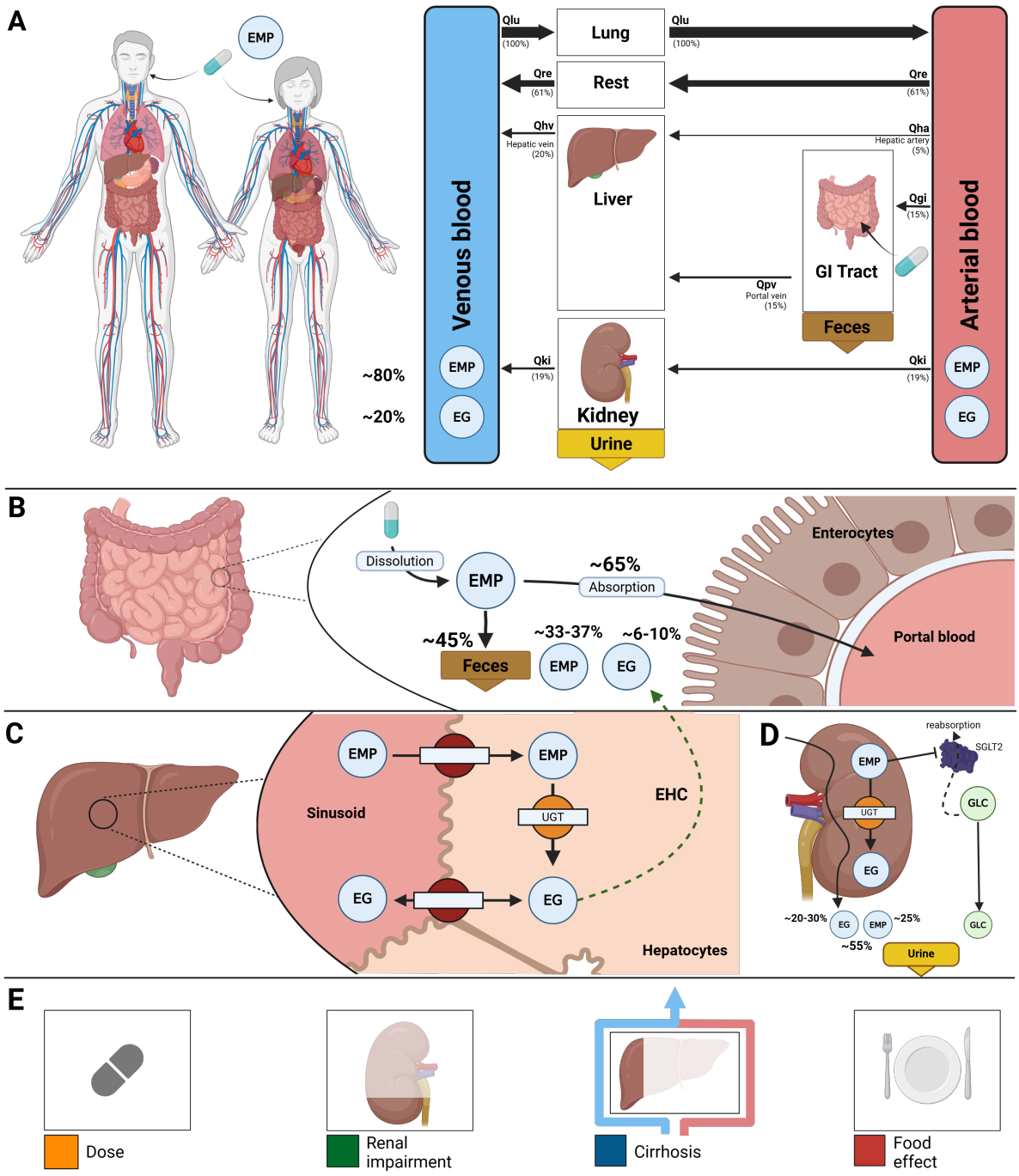

Figure 1. Whole-body PBPK/PD model of empagliflozin and key factors influencing its disposition. A) Whole-body model showing empagliflozin (EMP) administration, systemic circulation, and key organs (liver, kidney, GI tract) involved in metabolism, distribution, and excretion. **B)** Intestinal model illustrating EMP dissolution, absorption by enterocytes into portal blood, and fecal excretion of EMP and its glucuronide metabolite (EG). **C)** Hepatic model showing EMP uptake into hepatocytes, intracellular conversion to EG via UGT enzymes, and enterohepatic circulation (EHC) of EG back into the intestinal lumen. **D)** Renal model showing uptake and urinary excretion of EMP and EG, renal metabolic conversion of EMP to EG via UGT enzymes, and EMP-mediated inhibition of SGLT2, reducing renal glucose reabsorption and increasing urinary glucose excretion. **E)** Key factors influencing EMP disposition included in the model: administered dose, renal impairment, hepatic impairment, and food intake effects on absorption.

 doi:10.20944/preprints202603.1559.v1

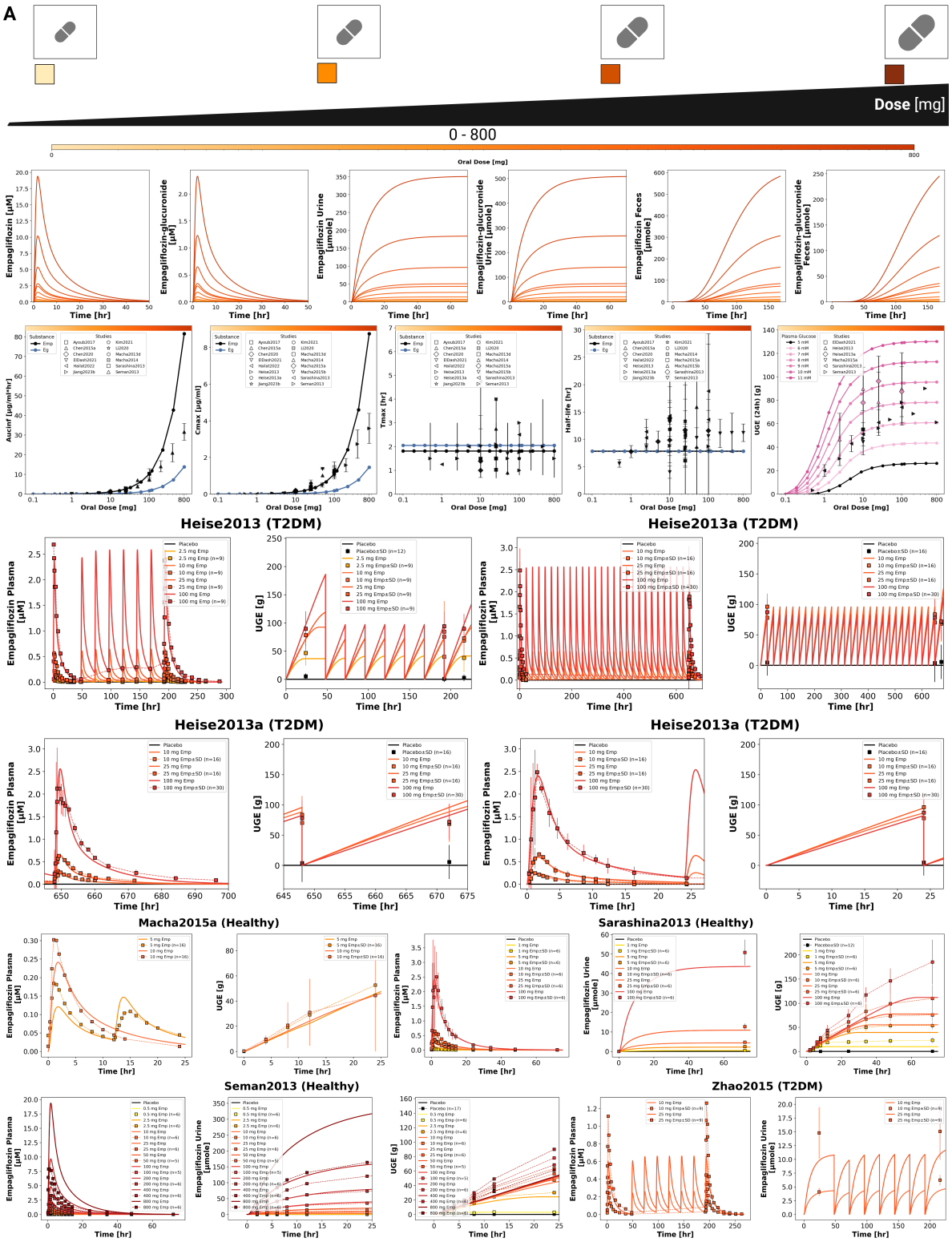

Figure 2. Dose-dependent pharmacokinetics and pharmacodynamics of empagliflozin. A) Oral dose range (0–800 mg). **B)** Pharmacokinetic time courses of empagliflozin and EG in plasma, urine, and feces. **C)** Pharmacokinetic parameters (AUC_{0-inf}, C_{max}, T_{max}, and half-life) for empagliflozin and EG, and 24 h UGE; observed parameters overlaid where available. **D)** Comparison of simulations with study data (Heise2013 [8], Heise2013a [53], Macha2015a [54], Sarashina2013 [55], Seman2013 [56], Zhao2015 [57]). Simulations are shown as solid lines and study data as symbols/dashed lines with SDs where available.

 doi:10.20944/preprints202603.1559.v1

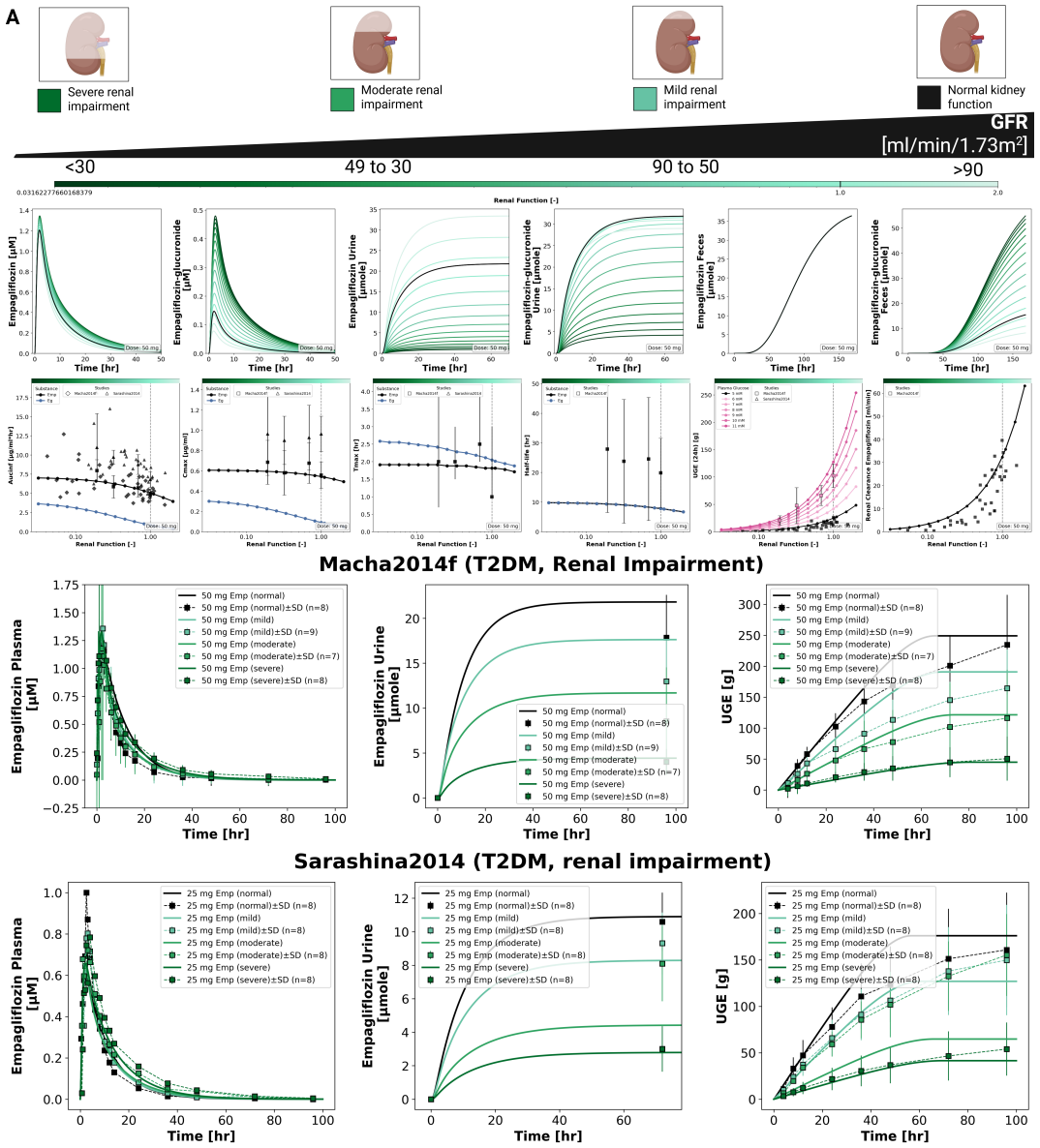

Figure 3. Effect of renal impairment on pharmacokinetics and pharmacodynamics of empagliflozin. A) Renal function categories from normal to severe impairment used in simulations. **B)** Pharmacokinetic time courses of empagliflozin and EG in plasma, urine, and feces. **C)** Pharmacokinetic parameters ($AUC_{0-\text{inf}}$, C_{max}, T_{max}, half-life, and renal clearance) for empagliflozin and EG, and 24 h UGE; observed parameters overlaid where available. **D)** Comparison of simulations with study data (Macha2014f [13], Sarashina2014 [14]). Simulations are shown as solid lines, and study data as symbols/dashed lines with SDs where available.

3.5. Hepatic Impairment

The effect of hepatic impairment on empagliflozin pharmacokinetics and pharmacodynamics is summarized in Figure 4. Simulations were performed across a continuous range of cirrhosis degree, with discrete categories corresponding to normal liver function and mild, moderate, and severe cirrhosis (CTP classes A, B, and C). With increasing hepatic impairment, empagliflozin and EG plasma exposure increased minimally, with $AUC_{0-\text{inf}}$ and C_{max} remaining nearly unchanged across cirrhosis severity. T_{max} was stable for both empagliflozin and EG across all hepatic function categories. Urinary excretion of both empagliflozin and EG increased slightly with higher cirrhosis degree.

The pharmacodynamic response was largely preserved across hepatic function states. UGE remained nearly unchanged with increasing cirrhosis severity, consistent with the predominantly renal mechanism of empagliflozin pharmacodynamics, which is independent of hepatic function.

 doi:10.20944/preprints202603.1559.v1

Simulated plasma concentration time courses and urinary excretion profiles for empagliflozin and EG under different degrees of hepatic impairment are shown together with clinical data from Macha2014b [15] and show good agreement.

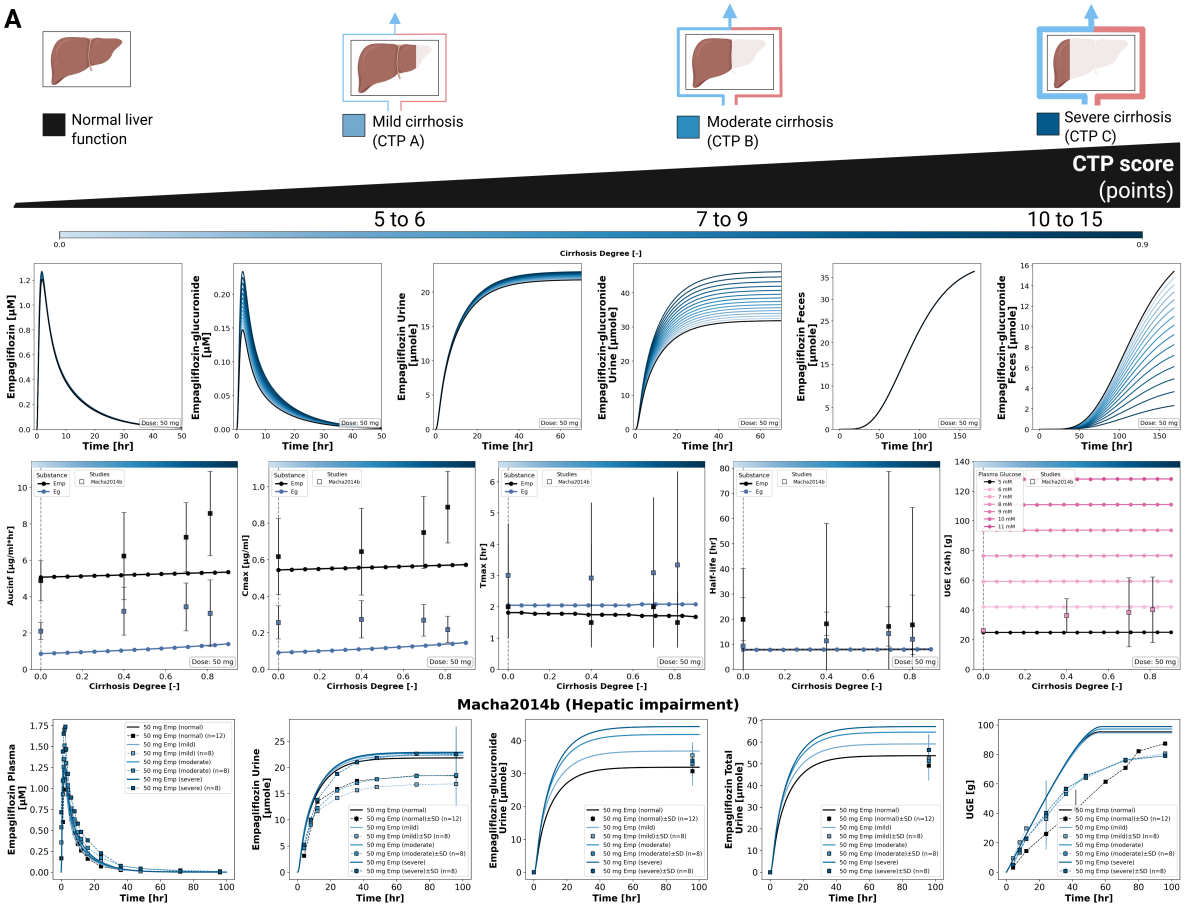

Figure 4. Effect of hepatic impairment on pharmacokinetics and pharmacodynamics of empagliflozin. A) Liver function categories used in simulations. **B)** Pharmacokinetic time courses of empagliflozin and EG in plasma, urine, and feces. **C)** Pharmacokinetic parameters ($AUC_{0-\mathrm{inf}}$, C_{max}, T_{max}, and half-life) for empagliflozin and EG, and 24 h UGE; observed parameters overlaid where available. **D)** Comparison of simulations with study data from Macha2014b [15]. Simulations are shown as solid lines, and study data as symbols/dashed lines with SDs where available.

3.6. Food Effect

The effect of food intake on empagliflozin pharmacokinetics and pharmacodynamics is summarized in Figure 5. Simulations were performed across a continuous range of absorption activity (0.1–1.5), with fasted and fed conditions corresponding to absorption scaling factors of 1.0 and 0.8, respectively. With decreasing absorption activity, C_{max} decreased and T_{max} increased, reflecting a slower and lower peak absorption under fed conditions. $AUC_{0-\mathrm{inf}}$ remained nearly unchanged across the full absorption activity range. EG plasma concentrations and urinary excretion followed the same pattern as the parent drug. Similarly, the model predicts that UGE is unaffected by food intake at all simulated plasma glucose levels. However, we have no clinical UGE data with which to compare our simulations.

Simulated empagliflozin plasma concentration time courses under fasted and fed conditions are shown together with clinical data from four studies (Seman2013 [56], Chen2020 [58], Hailat2022 [59], Li2020 [11]). Figure 5 retains Hailat2022, even though it was marked as an outlier. This is done for visual reference, as the general shape of the fasted and fed profiles remains informative in the context of other food-effect studies.

Table 1. Summary of studies for modeling. Overview of study identifiers, PubMed IDs, PK-DB IDs, administered substance, route, dosing, and subject characteristics, including health status (*H*), renal impairment (*RI*), hepatic impairment (*HI*), fasting status, type 2 diabetes (*T2*), urinary glucose excretion (*UGE*), fasting plasma glucose (*FPG*), renal threshold for glucose (*RTG*). *EMP P* = empagliflozin plasma, *EMP U* = empagliflozin urine, *EMP B* = empagliflozin bile, *EMP F* = empagliflozin feces

Study	PubMed	PK-DB	Substance	Route	Dosing	Dose [mg]	Fast	EMP P	EMP U	EMP B	EMP F	H	RI	HI	T2	UGE	FPG	RTG
Ayoub2017 [60]	28566743	PKDB00900	empagliflozin	oral	single	25	NR	✓				✓						
Brand2012 [61]	23054692	PKDB00902	empagliflozin	oral	multiple	50	NR	✓	✓			✓						
Chen2015a [62]	25547626	PKDB00930	empagliflozin, C14 empagliflozin	oral	single	50	NR	✓	✓		✓	✓				✓		
Chen2020 [58]	32498113	PKDB00901	empagliflozin	oral	single	10	fasting, fed	✓				✓					✓	
ElDash2021 [63]	34123370	PKDB00944	empagliflozin	oral	multiple	10	NR	✓	✓			✓				✓		
Friedrich2013 [64]	23328275	PKDB00916	empagliflozin	oral	multiple	50	NR	✓	✓			✓						
Hailat2022 [59]	35215305	PKDB00931	empagliflozin	oral	single	10, 25	fasted, fed	✓				✓						
Heise2013 [8]	23838841	PKDB00914	empagliflozin	oral	single, multiple	2.5, 10, 25, 100	NR	✓							✓	✓	✓	
Heise2013a [53]	23356556	PKDB00915	empagliflozin	oral	single, multiple	10.0, 25, 100	NR								✓	✓		
Heise2015 [65]	25636696	PKDB00852	empagliflozin	oral	single	25	NR					✓				✓		
Jiang2023b [66]	37521035	PKDB01000	empagliflozin	oral	single	25	fasted	✓				✓						
Kim2021 [67]	33953542	PKDB00996	empagliflozin	oral	multiple	25	fasted	✓				✓						
Kim2023 [68]	37282359	PKDB00927	empagliflozin	oral	multiple	25	fasted	✓				✓						
Laffel2018 [69]	29655290	PKDB01155	empagliflozin	oral	single	5, 10, 25		✓							✓	✓	✓	
Li2020 [11]	32799565	PKDB00995	empagliflozin	oral	single	25	fasted, fed	✓				✓						
Macha2013d [70]	23497760	PKDB01157	empagliflozin	oral	single, multiple	25	fasted	✓				✓						
Macha2013e [71]	23094794	PKDB01001	empagliflozin	oral	single	25	fasted	✓				✓						
Macha2014 [72]	24491572	PKDB01002	empagliflozin	oral	single	10, 25	fasted	✓				✓						
Macha2014b [15]	23859534	PKDB00938	empagliflozin	oral	single	50	fasted	✓	✓			✓		✓				
Macha2014f [13]	23859488	PKDB00939	empagliflozin	oral	single	50	NR	✓	✓			✓	✓		✓	✓		
Macha2015a [54]	26138865	PKDB00940	empagliflozin	oral	multiple	5, 10	fed	✓	✓			✓				✓		
Macha2015b [73]	26051874	PKDB01156	empagliflozin	oral	multiple	50	fasted	✓				✓						
Sarashina2013 [55]	23149871	PKDB00941	empagliflozin	oral	single	1, 5, 10, 25, 100	NR	✓	✓			✓				✓		
Sarashina2014 [14]	25199997	PKDB00942	empagliflozin	oral	single	25	NR	✓	✓				✓		✓	✓		
Seman2013 [56]	27121669	PKDB00943	empagliflozin	oral	single	0.5, 2.5, 10, 25, 50, 100, 200, 400, 800	NR, fasting, fed	✓	✓			✓				✓		
vanderAart-vanderBeek2020 [74]	32663790	PKDB00929	empagliflozin	oral	multiple	10	NR	✓							✓			
Zhao2015 [57]	26101175	PKDB00932	empagliflozin	oral	multiple	10, 25	fasted	✓	✓						✓	✓	✓	

 doi:10.20944/preprints202603.1559.v1

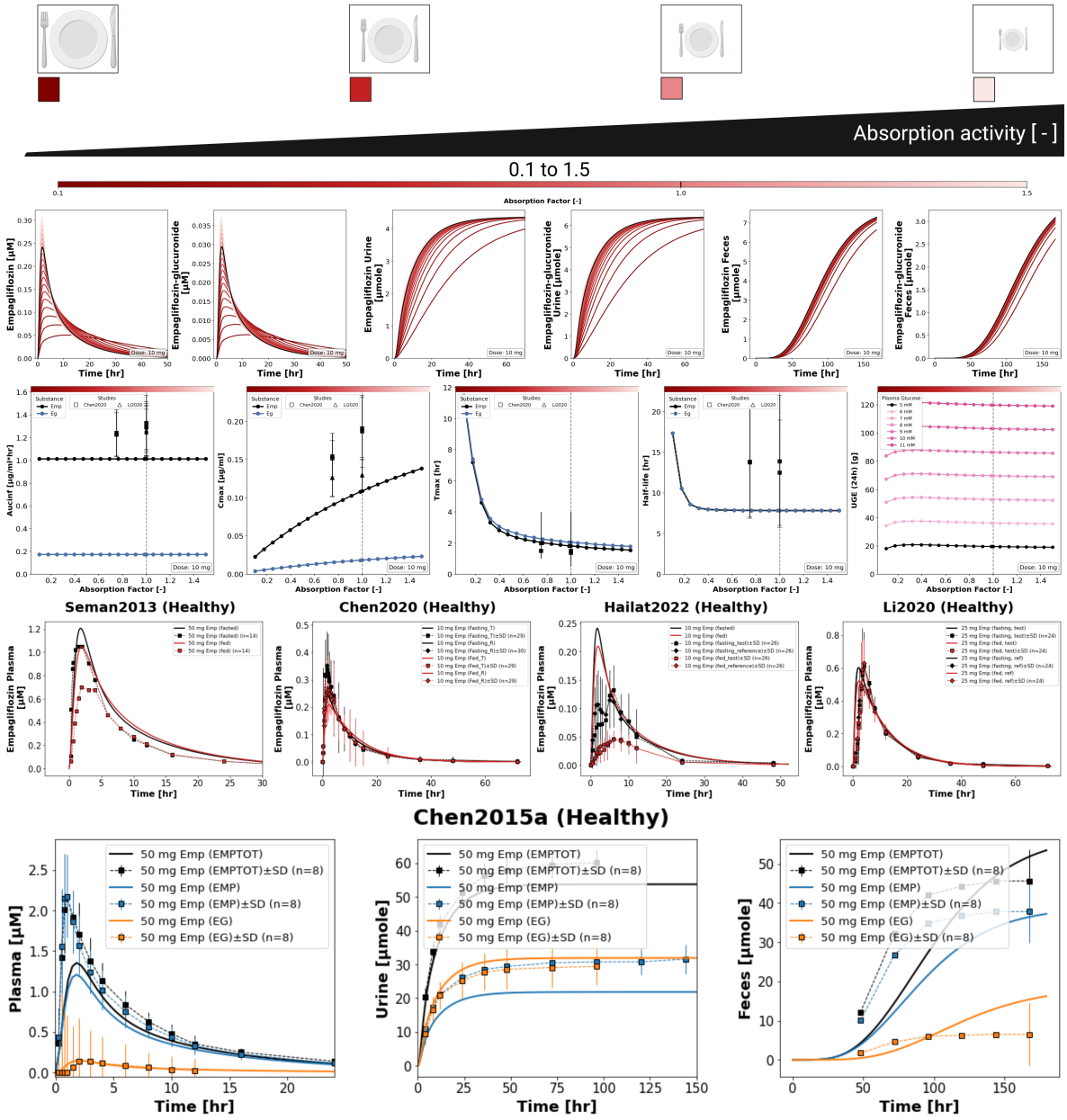

Figure 5. Effect of food intake (absorption) on pharmacokinetics and pharmacodynamics of empagliflozin. **A)** Absorption activity range used in simulations. **B)** Pharmacokinetic time courses of empagliflozin and EG in plasma, urine, and feces. **C)** Pharmacokinetic parameters (AUC_{0-inf}, C_{max}, T_{max}, and half-life) for empagliflozin and EG, and 24 h UGE; observed parameters overlaid where available. **D)** Comparison of simulations with study data (Seman2013 [56], Chen2020 [58], Hailat2022 [59], Li2020[11]). Simulations are shown as solid lines, and study data as symbols/dashed lines with SDs where available. Hailat2022 [59] is included for visual reference but was excluded from parameter optimization due to atypical double-peak absorption behavior and a probable unit inconsistency in the reported concentration values. **Note:** Chen2015a [62] is shown separately (bottom row) to show urinary and fecal excretion of parent drug and glucuronide metabolite; it is not a fasted/fed study and was included here to present excretion data.

4. Discussion

In this study, we established a comprehensive clinical dataset of empagliflozin pharmacokinetics and pharmacodynamics and used it to develop a mechanistic PBPK/PD digital twin. In total, 27 clinical studies were curated, covering a broad spectrum of dosing regimens and study populations, including healthy individuals, patients with T2DM, and cohorts with renal and hepatic impairment. Overall, data availability was sufficient for model development and evaluation, with consistent reporting of plasma concentration–time courses and urinary excretion across both single- and multiple-dose

 doi:10.20944/preprints202603.1559.v1

designs. Data on empagliflozin glucuronide plasma concentrations and fecal excretion were limited but sufficient to constrain the metabolite-related model components. No direct RTG measurements were available; however, UGE data were well represented across studies and dose levels, providing an adequate basis for calibration and evaluation of the pharmacodynamic model component.

The PBPK/PD framework integrates intestinal absorption, systemic distribution, hepatic metabolism, and renal elimination into a coherent representation of empagliflozin disposition and pharmacodynamic effect. Robust parameter optimization and good agreement between simulations and observed data across a wide range of studies and conditions support the reliability of the model. A key strength of this mechanistic approach is its ability to investigate scenarios that are difficult to address systematically in clinical trials, such as direct comparisons between renal and hepatic impairment, controlled exploration of dose-dependent behavior across physiological states, and the influence of food intake on absorption and exposure. Pharmacodynamic effects are driven by plasma empagliflozin concentrations through inhibition of SGLT2, resulting in modulation of the RTG and a mechanistic, physiologically interpretable link between drug exposure and UGE.

Two optimized parameters reached their upper bounds during parameter optimization: the biliary EG export rate constant in the liver (LI_EGBIEX_k) and the Michaelis constant for renal UGT-mediated glucuronidation (KI_EMP2EG_Km_emp). This likely reflects limited sensitivity of the available calibration data to these specific processes, as biliary EG excretion data are sparse and renal glucuronidation contributes only partially to total EG formation.

The simulations reproduced the expected dose-dependent pharmacokinetic and pharmacodynamic behavior of empagliflozin, with increasing doses leading to proportionally higher plasma exposure and greater UGE. Across the investigated dose range, time to maximum concentration and elimination half-life remained largely unchanged, consistent with dose-proportional kinetics. The modeled dose-dependent increase in UGE reflects progressive inhibition of renal glucose reabsorption and is consistent with the nonlinear exposure–response relationship reported in clinical studies. At extreme doses approaching 800 mg, model predictions showed a tendency to overestimate plasma exposure, which likely reflects the limits of linear scaling assumptions at concentrations well outside the therapeutic range; performance across clinically relevant dose levels was not affected.

The pharmacokinetics and pharmacodynamics of empagliflozin under conditions of hepatic impairment are less extensively characterized than in other clinical populations. Evaluation in this setting was constrained by the availability of clinical data, as only one study reported plasma concentration–time profiles alongside urinary excretion of both empagliflozin and its glucuronide metabolite, as well as UGE. Despite this limitation, model simulations were in good agreement with the available observations across all measured endpoints. Simulated plasma concentration–time profiles for empagliflozin and EG, urinary excretion, and UGE were all well reproduced across the range of hepatic impairment categories. The model predicted only modest increases in empagliflozin and EG plasma exposure with worsening hepatic dysfunction, likely because empagliflozin undergoes glucuronidation in both the liver and the kidney. As hepatic UGT activity declines, renal glucuronidation partially compensates, limiting the overall impact on systemic exposure. Furthermore, since the pharmacodynamic effect is driven by renal filtration and SGLT2 inhibition in the proximal tubule rather than by hepatic function, UGE remained largely preserved across cirrhosis severity. That said, conclusions drawn from this population should be interpreted with caution, as they rest on a single clinical study, and further data would strengthen confidence in model predictions for patients with liver disease.

Renal impairment represented an important source of variability in empagliflozin treatment response and had a pronounced influence on the pharmacodynamic outcome. Evaluation in this population was supported by two clinical studies, both reporting parent empagliflozin plasma concentration–time profiles, urinary excretion of empagliflozin, and UGE across categories of renal function; data on EG plasma concentrations or urinary excretion were not available from these studies. Model simulations were in good agreement with the clinical observations across all available endpoints. Parent empagliflozin plasma exposure changed only modestly with declining renal function, consistent with

 doi:10.20944/preprints202603.1559.v1

the presence of alternative clearance routes including hepatic metabolism, though these could not be directly verified against data in this setting. In contrast, urinary excretion of empagliflozin and UGE both declined markedly with worsening renal function, and these trends were well captured by the model across all impairment categories. With declining GFR, less glucose is delivered to the proximal tubule, reducing the substrate available for SGLT2 inhibition and thereby attenuating the pharmacodynamic response independent of drug exposure. Thus, renal function represents a key determinant of empagliflozin efficacy.

The effect of food intake on empagliflozin pharmacokinetics was evaluated across four clinical studies, all in healthy volunteers. Consistent with the published literature, fed conditions were associated with a lower and delayed peak plasma concentration compared to fasted administration, while overall exposure remained largely unchanged. These modest pharmacokinetic differences are generally considered not clinically meaningful, and empagliflozin can be administered irrespective of meals. Agreement between simulations and observed plasma profiles was reasonable across the available studies. Hailat2022 was excluded from parameter optimization due to atypical double-peak behavior and a likely unit inconsistency in the reported concentration values, and should be interpreted with caution. Direct evaluation of the simulated UGE response under fasted and fed conditions was not possible due to the lack of pharmacodynamic endpoints from the food effect studies. Simulations predicted that UGE is largely insensitive to the modest changes in absorption rate associated with food intake, consistent with the clinical understanding that glycemic efficacy is preserved regardless of prandial state.

Future work could focus on expanding the clinical data base for empagliflozin under conditions of organ impairment. For hepatic impairment, the current evaluation rests on a single study, and more comprehensive data, including pharmacodynamic endpoints such as UGE would allow a more complete assessment of model behavior in this population. For renal impairment, the available studies were restricted to single-dose designs and did not include EG measurements; multiple-dose data and metabolite profiles would further support model refinement and validation across the full range of renal function categories. More broadly, consistent and standardized reporting of both pharmacokinetic and pharmacodynamic endpoints across organ impairment studies would substantially improve the utility of mechanistic PBPK/PD frameworks for characterizing drug behavior in patients with altered organ function.

Beyond the pharmacological findings, this work also addresses a broader challenge in computational pharmacology and systems biology related to model transparency and reproducibility. A substantial fraction of published PBPK models cannot be independently reproduced because essential components such as model equations, executable code, and curated calibration datasets are not publicly available [29,30], which limits independent verification and restricts reuse, extension, and cumulative model development within the field. To address this, reproducibility and accessibility were treated as core design principles throughout this work. The complete modeling framework, including the SBML model, simulation scripts, and curated clinical datasets, is openly available and structured in accordance with FAIR principles [34,75], enabling independent reproduction, transparent evaluation, and systematic reuse across different contexts. All resources are released under permissive MIT and CC-BY licenses, lowering barriers to reuse in both academic and industrial settings and allowing straightforward integration into existing workflows.

In summary, this PBPK/PD digital twin of empagliflozin integrates diverse clinical data into a mechanistic framework that captures pharmacokinetic and pharmacodynamic behavior across a wide range of dosing regimens and patient populations. The model provides quantitative insight into dose dependency and the effects of renal impairment, hepatic impairment, and food intake on drug exposure and response, supporting the analysis of variability under clinically relevant conditions. Full open access to the model, simulation code, and curated datasets establishes a transparent and reproducible reference framework that supports independent validation, reuse, and future extension of empagliflozin PBPK/PD modeling efforts.

 doi:10.20944/preprints202603.1559.v1

Supplementary Materials: The following supporting information can be downloaded at the website of this paper posted on Preprints.org.

Author Contributions: Conceptualization, J.A. and M.K.; methodology, J.A., M.E., and M.K.; software, J.A., M.E., and M.K.; validation, J.A., M.E., and M.K.; formal analysis, J.A., M.E., and M.K.; data curation, J.A., M.B. and M.K.; writing—original draft preparation, M.E.; writing—review and editing, J.A., M.E., M.B. and M.K.; visualization, J.A., M.E., M.B. and M.K.; supervision, M.K.; project administration, M.K.; funding acquisition, M.K. All authors have read and agreed to the published version of the manuscript.

Funding: M.K. was supported by the Federal Ministry of Research, Technology and Space (BMFTR, Germany) within ATLAS by grant number 031L0304B and by the German Research Foundation (DFG) by the DFG grant number 436883643 and 465194077. M.E. was supported by the DFG under grant number 465194077.

Institutional Review Board Statement: Not applicable.

Informed Consent Statement: Not applicable.

Data Availability Statement: All curated pharmacokinetic data are publicly available in the PK-DB database (https://pk-db.com). The model and all associated materials (simulation scripts, parameters, and documentation) are publicly available in SBML format under a CC-BY 4.0 license at https://github.com/matthiaskoenig/empagliflozin-model [46].

Acknowledgments: This work was supported by the BMBF-funded de.NBI Cloud within the German Network for Bioinformatics Infrastructure (de.NBI) (031A537B, 031A533A, 031A538A, 031A533B, 031A535A, 031A537C, 031A534A, 031A532B). Figures were created in BioRender. König, M. (2026) https://BioRender.com/48jro1s.

Conflicts of Interest: The authors declare no conflicts of interest.

References

1. American Diabetes Association Professional Practice Committee. 2. Diagnosis and Classification of Diabetes: Standards of Care in Diabetes-2024. *Diabetes Care* **2024**, *47*, S20–S42. https://doi.org/10.2337/dc24-S002.
2. Institute for Health Metrics and Evaluation (IHME). Global Burden of Disease 2023: Findings from the GBD 2023 Study. Technical report, Institute for Health Metrics and Evaluation, Seattle, WA, 2025. Licensed under CC BY-NC-ND 4.0.
3. Vallon, V. Glucose Transporters in the Kidney in Health and Disease. *Pflugers Archiv: European Journal of Physiology* **2020**, *472*, 1345–1370. https://doi.org/10.1007/s00424-020-02361-w.
4. DeFronzo, R.A.; Hompesch, M.; Kasichayanula, S.; Liu, X.; Hong, Y.; Pfister, M.; Morrow, L.A.; Leslie, B.R.; Boulton, D.W.; Ching, A.; et al. Characterization of Renal Glucose Reabsorption in Response to Dapagliflozin in Healthy Subjects and Subjects with Type 2 Diabetes. *Diabetes Care* **2013**, *36*, 3169–3176. https://doi.org/10.2337/dc13-0387.
5. Nisly, S.A.; Kolanczyk, D.M.; Walton, A.M. Canagliflozin, a New Sodium-Glucose Cotransporter 2 Inhibitor, in the Treatment of Diabetes. *American journal of health-system pharmacy : AJHP : official journal of the American Society of Health-System Pharmacists* **2013**, *70*, 311–319. https://doi.org/10.2146/ajhp110514.
6. Deeks, E.D.; Scheen, A.J. Canagliflozin: A Review in Type 2 Diabetes. *Drugs* **2017**, *77*, 1577–1592. https://doi.org/10.1007/s40265-017-0801-6.
7. Mahayni, H.; Dorantes, A. Clinical Pharmacology and Biopharmaceutics Review: Empagliflozin (BI 10773), NDA 204-629. Clinical Pharmacology and Biopharmaceutics Review NDA 204629Orig1s000, U.S. Food and Drug Administration, Center for Drug Evaluation and Research, Silver Spring, MD, 2014. Trade name: Jardiance. Application for adjunct therapy in type 2 diabetes mellitus. Reference ID: 3596106.
8. Heise, T.; Seman, L.; Macha, S.; Jones, P.; Marquart, A.; Pinnetti, S.; Woerle, H.J.; Dugi, K. Safety, Tolerability, Pharmacokinetics, and Pharmacodynamics of Multiple Rising Doses of Empagliflozin in Patients with Type 2 Diabetes Mellitus. *Diabetes therapy : research, treatment and education of diabetes and related disorders* **2013**, *4*, 331–345. https://doi.org/10.1007/s13300-013-0030-2.
9. Scheen, A.J. Pharmacokinetic and Pharmacodynamic Profile of Empagliflozin, a Sodium Glucose Co-Transporter 2 Inhibitor. *Clinical pharmacokinetics* **2014**, *53*, 213–225. https://doi.org/10.1007/s40262-013-0126-x.

 doi:10.20944/preprints202603.1559.v1

10. Macha, S.; Jungnik, A.; Hohl, K.; Hobson, D.; Salsali, A.; Woerle, H.J. Effect of Food on the Pharmacokinetics of Empagliflozin, a Sodium Glucose Cotransporter 2 (SGLT2) Inhibitor, and Assessment of Dose Proportionality in Healthy Volunteers. *International journal of clinical pharmacology and therapeutics* **2013**, *51*, 873–879. https://doi.org/10.5414/cp201948.
11. Li, X.; Liu, L.; Deng, Y.; Li, Y.; Zhang, P.; Wang, Y.; Xu, B. Pharmacokinetics and Bioequivalence of a Generic Empagliflozin Tablet versus a Brand-Named Product and the Food Effects in Healthy Chinese Subjects. *Drug development and industrial pharmacy* **2020**, *46*, 1487–1494. https://doi.org/10.1080/03639045.2020.1810263.
12. Ndefo, U.A.; Anidiobi, N.O.; Basheer, E.; Eaton, A.T. Empagliflozin (Jardiance): A Novel SGLT2 Inhibitor for the Treatment of Type-2 Diabetes. *P & T: A Peer-Reviewed Journal for Formulary Management* **2015**, *40*, 364–368.
13. Macha, S.; Mattheus, M.; Halabi, A.; Pinnetti, S.; Woerle, H.J.; Broedl, U.C. Pharmacokinetics, Pharmacodynamics and Safety of Empagliflozin, a Sodium Glucose Cotransporter 2 (SGLT2) Inhibitor, in Subjects with Renal Impairment. *Diabetes, obesity & metabolism* **2014**, *16*, 215–222. https://doi.org/10.1111/dom.12182.
14. Sarashina, A.; Ueki, K.; Sasaki, T.; Tanaka, Y.; Koiwai, K.; Sakamoto, W.; Woerle, H.J.; Salsali, A.; Broedl, U.C.; Macha, S. Effect of Renal Impairment on the Pharmacokinetics, Pharmacodynamics, and Safety of Empagliflozin, a Sodium Glucose Cotransporter 2 Inhibitor, in Japanese Patients with Type 2 Diabetes Mellitus. *Clinical therapeutics* **2014**, *36*, 1606–1615. https://doi.org/10.1016/j.clinthera.2014.08.001.
15. Macha, S.; Rose, P.; Mattheus, M.; Cinca, R.; Pinnetti, S.; Broedl, U.C.; Woerle, H.J. Pharmacokinetics, Safety and Tolerability of Empagliflozin, a Sodium Glucose Cotransporter 2 Inhibitor, in Patients with Hepatic Impairment. *Diabetes, obesity & metabolism* **2014**, *16*, 118–123. https://doi.org/10.1111/dom.12183.
16. Baron, K.T.; Macha, S.; Broedl, U.C.; Nock, V.; Retlich, S.; Riggs, M. Population Pharmacokinetics and Exposure-Response (Efficacy and Safety/Tolerability) of Empagliflozin in Patients with Type 2 Diabetes. *Diabetes therapy : research, treatment and education of diabetes and related disorders* **2016**, *7*, 455–471. https://doi.org/10.1007/s13300-016-0174-y.
17. Riggs, M.M.; Staab, A.; Seman, L.; MacGregor, T.R.; Bergsma, T.T.; Gastonguay, M.R.; Macha, S. Population Pharmacokinetics of Empagliflozin, a Sodium Glucose Cotransporter 2 Inhibitor, in Patients with Type 2 Diabetes. *Journal of clinical pharmacology* **2013**, *53*, 1028–1038. https://doi.org/10.1002/jcph.147.
18. Riggs, M.M.; Seman, L.J.; Staab, A.; MacGregor, T.R.; Gillespie, W.; Gastonguay, M.R.; Woerle, H.J.; Macha, S. Exposure-Response Modelling for Empagliflozin, a Sodium Glucose Cotransporter 2 (SGLT2) Inhibitor, in Patients with Type 2 Diabetes. *British journal of clinical pharmacology* **2014**, *78*, 1407–1418. https://doi.org/10.1111/bcp.12453.
19. Fayette, L.; Sailer, M.O.; Perez-Pitarch, A. Pharmacometrics Enhanced Bayesian Borrowing Approach to Improve Clinical Trial Efficiency: Case of Empagliflozin in Type 2 Diabetes. *CPT: pharmacometrics & systems pharmacology* **2023**, *12*, 1386–1397. https://doi.org/10.1002/psp4.13035.
20. Jiang, X.; Yu, K.S.; Nam, D.H.; Oh, J. A Population Pharmacokinetic Study to Compare a Novel Empagliflozin L-Proline Formulation with Its Conventional Formulation in Healthy Subjects. *Pharmaceuticals (Basel, Switzerland)* **2024**, *17*. https://doi.org/10.3390/ph17040522.
21. Mondick, J.; Riggs, M.; Kaspers, S.; Soleymanlou, N.; Marquard, J.; Nock, V. Population Pharmacokinetic-Pharmacodynamic Analysis to Characterize the Effect of Empagliflozin on Renal Glucose Threshold in Patients With Type 1 Diabetes Mellitus. *Journal of clinical pharmacology* **2018**, *58*, 640–649. https://doi.org/10.1002/jcph.1051.
22. Perkins, B.A.; Soleymanlou, N.; Rosenstock, J.; Skyler, J.S.; Laffel, L.M.; Liesenfeld, K.H.; Neubacher, D.; Riggs, M.M.; Johnston, C.K.; Eudy-Byrne, R.J.; et al. Low-Dose Empagliflozin as Adjunct-to-Insulin Therapy in Type 1 Diabetes: A Valid Modelling and Simulation Analysis to Confirm Efficacy. *Diabetes, obesity & metabolism* **2020**, *22*, 427–433. https://doi.org/10.1111/dom.13945.
23. Yao, X.; Zhou, J.; Song, L.; Ren, Y.; Hu, P.; Liu, D. A Model-Based Meta Analysis Study of Sodium Glucose Co-Transporter-2 Inhibitors. *CPT: pharmacometrics & systems pharmacology* **2023**, *12*, 487–499. https://doi.org/10.1002/psp4.12934.
24. Guo, G.; Ke, M.; Xu, J.; Wu, W.; Chen, J.; Ke, C.; Huang, P.; Lin, C. Physiologically Based Pharmacokinetic Model of Sodium-Glucose Cotransporter 2 Inhibitors Predicted Pharmacokinetics and Pharmacodynamics to Explore Dosage Regimen for Patients with Type 2 Diabetes Mellitus and Renal Insufficiency. *Frontiers in Pharmacology* **2025**, *16*, 1520268. https://doi.org/10.3389/fphar.2025.1520268.
25. Ping, X.; Wang, G.; Gao, D. Mechanistic Modeling of Empagliflozin: Predicting Pharmacokinetics, Urinary Glucose Excretion, and Investigating Compensatory Role of SGLT1 in Renal Glucose Reabsorption. *Journal of clinical pharmacology* **2024**, *64*, 672–684. https://doi.org/10.1002/jcph.2413.

 doi:10.20944/preprints202603.1559.v1

26. Zhang, Y.; Xie, P.; Li, Y.; Chen, Z.; Shi, A. Mechanistic Evaluation of the Inhibitory Effect of Four SGLT-2 Inhibitors on SGLT 1 and SGLT 2 Using Physiologically Based Pharmacokinetic (PBPK) Modeling Approaches. *Frontiers in pharmacology* **2023**, *14*, 1142003. https://doi.org/10.3389/fphar.2023.1142003.
27. Yakovleva, T.; Sokolov, V.; Chu, L.; Tang, W.; Greasley, P.J.; Peilot Sjögren, H.; Johansson, S.; Peskov, K.; Helmlinger, G.; Boulton, D.W.; et al. Comparison of the Urinary Glucose Excretion Contributions of SGLT2 and SGLT1: A Quantitative Systems Pharmacology Analysis in Healthy Individuals and Patients with Type 2 Diabetes Treated with SGLT2 Inhibitors. *Diabetes, Obesity & Metabolism* **2019**, *21*, 2684–2693. https://doi.org/10.1111/dom.13858.
28. Hosny, N.M.; GadAllah, M.I.; Qayed, W.S. Combined Experimental/Computational Aspects for the Molecular Interaction of Empagliflozin with Bovine Serum Albumin: Quantification and Application to Human Plasma. *Luminescence : the journal of biological and chemical luminescence* **2023**, *38*, 1449–1457. https://doi.org/10.1002/bio.4526.
29. Tiwari, K.; Kananathan, S.; Roberts, M.G.; Meyer, J.P.; Sharif Shohan, M.U.; Xavier, A.; Maire, M.; Zyoud, A.; Men, J.; Ng, S.; et al. Reproducibility in Systems Biology Modelling. *Molecular Systems Biology* **2021**, *17*, e9982. https://doi.org/10.15252/msb.20209982.
30. Domínguez-Romero, E.; Mazurenko, S.; Scheringer, M.; Martins Dos Santos, V.A.P.; Evelo, C.T.; Anton, M.; Hancock, J.M.; Županič, A.; Suarez-Diez, M. Making PBPK Models More Reproducible in Practice. *Briefings in Bioinformatics* **2024**, *25*, bbae569. https://doi.org/10.1093/bib/bbae569.
31. Jones, H.; Rowland-Yeo, K. Basic Concepts in Physiologically Based Pharmacokinetic Modeling in Drug Discovery and Development. *CPT: Pharmacometrics & Systems Pharmacology* **2013**, *2*, 1–12. https://doi.org/10.1038/psp.2013.41.
32. Sager, J.E.; Yu, J.; Ragueneau-Majlessi, I.; Isoherranen, N. Physiologically Based Pharmacokinetic (PBPK) Modeling and Simulation Approaches: A Systematic Review of Published Models, Applications, and Model Verification. *Drug Metabolism and Disposition* **2015**, *43*, 1823–1837. https://doi.org/10.1124/dmd.115.065920.
33. Hartmanshenn, C.; Scherholz, M.; Androulakis, I.P. Physiologically-Based Pharmacokinetic Models: Approaches for Enabling Personalized Medicine. *Journal of Pharmacokinetics and Pharmacodynamics* **2016**, *43*, 481–504. https://doi.org/10.1007/s10928-016-9492-y.
34. Wilkinson, M.D.; Dumontier, M.; Aalbersberg, I.J.J.; Appleton, G.; Axton, M.; Baak, A.; Blomberg, N.; Boiten, J.W.; da Silva Santos, L.B.; Bourne, P.E.; et al. The FAIR Guiding Principles for Scientific Data Management and Stewardship. *Scientific Data* **2016**, *3*, 160018. https://doi.org/10.1038/sdata.2016.18.
35. Hucka, M.; Bergmann, F.T.; Chaouiya, C.; Dräger, A.; Hoops, S.; Keating, S.M.; König, M.; Novère, N.L.; Myers, C.J.; Olivier, B.G.; et al. The Systems Biology Markup Language (SBML): Language Specification for Level 3 Version 2 Core Release 2. *Journal of Integrative Bioinformatics* **2019**, *16*. https://doi.org/10.1515/jib-2019-0021.
36. Gonzalez Hernandez, F.; Carter, S.J.; Iso-Sipilä, J.; Goldsmith, P.; Almousa, A.A.; Gastine, S.; Lilaonitkul, W.; Kloprogge, F.; Standing, J.F. An Automated Approach to Identify Scientific Publications Reporting Pharmacokinetic Parameters. *Wellcome Open Research* **2021**, *6*, 88. https://doi.org/10.12688/wellcomeopenres.16718.1.
37. Grzegorzewski, J.; Brandhorst, J.; Green, K.; Eleftheriadou, D.; Duport, Y.; Barthorscht, F.; Köller, A.; Ke, D.Y.J.; De Angelis, S.; König, M. PK-DB: Pharmacokinetics Database for Individualized and Stratified Computational Modeling. *Nucleic Acids Research* **2021**, *49*, D1358–D1364. https://doi.org/10.1093/nar/gkaa990.
38. Rohatgi, A. WebPlotDigitizer, 2024.
39. Keating, S.M.; Waltemath, D.; König, M.; Zhang, F.; Dräger, A.; Chaouiya, C.; Bergmann, F.T.; Finney, A.; Gillespie, C.S.; Helikar, T.; et al. SBML Level 3: An Extensible Format for the Exchange and Reuse of Biological Models. *Molecular Systems Biology* **2020**, *16*, e9110. https://doi.org/10.15252/msb.20199110.
40. König, M. Sbmlutils: Python Utilities for SBML. Zenodo, 2026. https://doi.org/10.5281/zenodo.18207772.
41. König, M.; Dräger, A.; Holzhütter, H.G. CySBML: A Cytoscape Plugin for SBML. *Bioinformatics (Oxford, England)* **2012**, *28*, 2402–2403, [22772946]. https://doi.org/10.1093/bioinformatics/bts432.
42. König, M. Cy3sbml - SBML for Cytoscape. Zenodo, 2025. https://doi.org/10.5281/zenodo.15009089.
43. König, M. Sbmlsim: SBML Simulation Made Easy. Zenodo, 2026. https://doi.org/10.5281/zenodo.18452043.
44. Somogyi, E.T.; Bouteiller, J.M.; Glazier, J.A.; König, M.; Medley, J.K.; Swat, M.H.; Sauro, H.M. libRoadRunner: A High Performance SBML Simulation and Analysis Library. *Bioinformatics (Oxford, England)* **2015**, *31*, 3315–3321. https://doi.org/10.1093/bioinformatics/btv363.
45. Welsh, C.; Xu, J.; Smith, L.; König, M.; Choi, K.; Sauro, H.M. libRoadRunner 2.0: A High Performance SBML Simulation and Analysis Library. *Bioinformatics* **2023**, *39*, btac770. https://doi.org/10.1093/bioinformatics/btac770.

 doi:10.20944/preprints202603.1559.v1

46. Alejandro, J.; Elias, M.; König, M. Physiologically Based Pharmacokinetic/ Pharmacodynamic (PBPK/PD) Model of Empagliflozin. Zenodo, 2026. https://doi.org/10.5281/zenodo.19087605.
47. Stevens, P.E.; Ahmed, S.B.; Carrero, J.J.; Foster, B.; Francis, A.; Hall, R.K.; Herrington, W.G.; Hill, G.; Inker, L.A.; Kazancıoğlu, R.; et al. KDIGO 2024 Clinical Practice Guideline for the Evaluation and Management of Chronic Kidney Disease. *Kidney International* **2024**, *105*, S117–S314. https://doi.org/10.1016/j.kint.2023.10.018.
48. Mallol, B.S.; Grzegorzewski, J.; Tautenhahn, H.M.; König, M. Insights into Intestinal P-glycoprotein Function Using Talinolol: A PBPK Modeling Approach, 2023. https://doi.org/10.1101/2023.11.21.568168.
49. Child, C.G.; Turcotte, J.G. Surgery and Portal Hypertension. *Major Problems in Clinical Surgery* **1964**, *1*, 1–85.
50. Pugh, R.N.; Murray-Lyon, I.M.; Dawson, J.L.; Pietroni, M.C.; Williams, R. Transection of the Oesophagus for Bleeding Oesophageal Varices. *The British Journal of Surgery* **1973**, *60*, 646–649. https://doi.org/10.1002/bjs.1800600817.
51. Köller, A.; Grzegorzewski, J.; Tautenhahn, H.M.; König, M. Prediction of Survival After Partial Hepatectomy Using a Physiologically Based Pharmacokinetic Model of Indocyanine Green Liver Function Tests. *Frontiers in physiology* **2021**, *12*, 730418.
52. Köller, A.; Grzegorzewski, J.; König, M. Physiologically Based Modeling of the Effect of Physiological and Anthropometric Variability on Indocyanine Green Based Liver Function Tests. *Frontiers in Physiology* **2021**, p. 2043.
53. Heise, T.; Seewaldt-Becker, E.; Macha, S.; Hantel, S.; Pinnetti, S.; Seman, L.; Woerle, H.J. Safety, Tolerability, Pharmacokinetics and Pharmacodynamics Following 4 Weeks' Treatment with Empagliflozin Once Daily in Patients with Type 2 Diabetes. *Diabetes, obesity & metabolism* **2013**, *15*, 613–621. https://doi.org/10.1111/dom.12073.
54. Macha, S.; Brand, T.; Meinicke, T.; Link, J.; Broedl, U.C. Pharmacokinetics and Pharmacodynamics of Twice Daily and Once Daily Regimens of Empagliflozin in Healthy Subjects. *Clinical therapeutics* **2015**, *37*, 1789–1796. https://doi.org/10.1016/j.clinthera.2015.06.003.
55. Sarashina, A.; Koiwai, K.; Seman, L.J.; Yamamura, N.; Taniguchi, A.; Negishi, T.; Sesoko, S.; Woerle, H.J.; Dugi, K.A. Safety, Tolerability, Pharmacokinetics and Pharmacodynamics of Single Doses of Empagliflozin, a Sodium Glucose Cotransporter 2 (SGLT2) Inhibitor, in Healthy Japanese Subjects. *Drug metabolism and pharmacokinetics* **2013**, *28*, 213–219. https://doi.org/10.2133/dmpk.dmpk-12-rg-082.
56. Seman, L.; Macha, S.; Nehmiz, G.; Simons, G.; Ren, B.; Pinnetti, S.; Woerle, H.J.; Dugi, K. Empagliflozin (BI 10773), a Potent and Selective SGLT2 Inhibitor, Induces Dose-Dependent Glucosuria in Healthy Subjects. *Clinical pharmacology in drug development* **2013**, *2*, 152–161. https://doi.org/10.1002/cpdd.16.
57. Zhao, X.; Cui, Y.; Zhao, S.; Lang, B.; Broedl, U.C.; Salsali, A.; Pinnetti, S.; Macha, S. Pharmacokinetic and Pharmacodynamic Properties and Tolerability of Single- and Multiple-Dose Once-daily Empagliflozin, a Sodium Glucose Cotransporter 2 Inhibitor, in Chinese Patients With Type 2 Diabetes Mellitus. *Clinical therapeutics* **2015**, *37*, 1493–1502. https://doi.org/10.1016/j.clinthera.2015.05.001.
58. Chen, G.; Zhang, D.; Du, A.; Zhang, Y.; Zhang, Y.; Zhang, L.; Zang, S.; Liu, X.; Wang, Z.; Zhen, H.; et al. Pharmacokinetics, Safety, and Bioequivalence of Two Empagliflozin Formulations after Single Oral Administration under Fasting and Fed Conditions in Healthy Chinese Subjects: An Open-label Randomized Single-dose Two-sequence, Two-treatment, Two-period Crossover Study. *Pharmacotherapy* **2020**, *40*, 623–631. https://doi.org/10.1002/phar.2432.
59. Hailat, M.; Zakaraya, Z.; Al-Ani, I.; Meanazel, O.A.; Al-Shdefat, R.; Anwer, M.K.; Saadh, M.J.; Abu Dayyih, W. Pharmacokinetics and Bioequivalence of Two Empagliflozin, with Evaluation in Healthy Jordanian Subjects under Fasting and Fed Conditions. *Pharmaceuticals (Basel, Switzerland)* **2022**, *15*. https://doi.org/10.3390/ph15020193.
60. Ayoub, B.M.; Mowaka, S.; Elzanfaly, E.S.; Ashoush, N.; Elmazar, M.M.; Mousa, S.A. Pharmacokinetic Evaluation of Empagliflozin in Healthy Egyptian Volunteers Using LC-MS/MS and Comparison with Other Ethnic Populations. *Scientific reports* **2017**, *7*, 2583. https://doi.org/10.1038/s41598-017-02895-7.
61. Brand, T.; Macha, S.; Mattheus, M.; Pinnetti, S.; Woerle, H.J. Pharmacokinetics of Empagliflozin, a Sodium Glucose Cotransporter-2 (SGLT-2) Inhibitor, Coadministered with Sitagliptin in Healthy Volunteers. *Advances in therapy* **2012**, *29*, 889–899. https://doi.org/10.1007/s12325-012-0055-3.
62. Chen, L.Z.; Jungnik, A.; Mao, Y.; Philip, E.; Sharp, D.; Unseld, A.; Seman, L.; Woerle, H.J.; Macha, S. Biotransformation and Mass Balance of the SGLT2 Inhibitor Empagliflozin in Healthy Volunteers. *Xenobiotica; the fate of foreign compounds in biological systems* **2015**, *45*, 520–529. https://doi.org/10.3109/00498254.2014.999141.

 doi:10.20944/preprints202603.1559.v1

63. ElDash, R.M.; Raslan, M.A.; Shaheen, S.M.; Sabri, N.A. The Effect of Morning versus Evening Administration of Empagliflozin on Its Pharmacokinetics and Pharmacodynamics Characteristics in Healthy Adults: A Two-Way Crossover, Non-Randomised Trial. *F1000Research* **2021**, *10*, 321. https://doi.org/10.12688/f1000research.51114.1.
64. Friedrich, C.; Metzmann, K.; Rose, P.; Mattheus, M.; Pinnetti, S.; Woerle, H.J. A Randomized, Open-Label, Crossover Study to Evaluate the Pharmacokinetics of Empagliflozin and Linagliptin after Coadministration in Healthy Male Volunteers. *Clinical therapeutics* **2013**, *35*, A33–42. https://doi.org/10.1016/j.clinthera.2012.12.002.
65. Heise, T.; Mattheus, M.; Woerle, H.J.; Broedl, U.C.; Macha, S. Assessing Pharmacokinetic Interactions between the Sodium Glucose Cotransporter 2 Inhibitor Empagliflozin and Hydrochlorothiazide or Torasemide in Patients with Type 2 Diabetes Mellitus: A Randomized, Open-Label, Crossover Study. *Clinical therapeutics* **2015**, *37*, 793–803. https://doi.org/10.1016/j.clinthera.2014.12.018.
66. Jiang, X.; Bae, S.; Yoon, D.Y.; Park, S.J.; Oh, J.; Cho, J.Y.; Yu, K.S. Comparison of the Pharmacokinetics, Safety, and Tolerability of Two Empagliflozin Formulations in Healthy Korean Subjects. *Drug design, development and therapy* **2023**, *17*, 2137–2145. https://doi.org/10.2147/DDDT.S409368.
67. Kim, Y.K.; Hwang, J.G.; Park, M.K. No Relevant Pharmacokinetic Drug-Drug Interaction Between the Sodium-Glucose Co-Transporter-2 Inhibitor Empagliflozin and Lobeglitazone, a Peroxisome Proliferator-Activated Receptor-γ Agonist, in Healthy Subjects. *Drug design, development and therapy* **2021**, *15*, 1725–1734. https://doi.org/10.2147/DDDT.S302215.
68. Kim, D.; Choi, M.; Jin, B.H.; Hong, T.; Kim, C.O.; Yoo, B.W.; Park, M.S. Pharmacokinetic and Pharmacodynamic Drug-Drug Interactions between Evogliptin and Empagliflozin or Dapagliflozin in Healthy Male Volunteers. *Clinical and translational science* **2023**, *16*, 1469–1478. https://doi.org/10.1111/cts.13566.
69. Laffel, L.M.B.; Tamborlane, W.V.; Yver, A.; Simons, G.; Wu, J.; Nock, V.; Hobson, D.; Hughan, K.S.; Kaspers, S.; Marquard, J. Pharmacokinetic and Pharmacodynamic Profile of the Sodium-Glucose Co-Transporter-2 Inhibitor Empagliflozin in Young People with Type 2 Diabetes: A Randomized Trial. *Diabetic medicine : a journal of the British Diabetic Association* **2018**, *35*, 1096–1104. https://doi.org/10.1111/dme.13629.
70. Macha, S.; Sennewald, R.; Rose, P.; Schoene, K.; Pinnetti, S.; Woerle, H.J.; Broedl, U.C. Lack of Clinically Relevant Drug-Drug Interaction between Empagliflozin, a Sodium Glucose Cotransporter 2 Inhibitor, and Verapamil, Ramipril, or Digoxin in Healthy Volunteers. *Clinical therapeutics* **2013**, *35*, 226–235. https://doi.org/10.1016/j.clinthera.2013.02.015.
71. Macha, S.; Rose, P.; Mattheus, M.; Pinnetti, S.; Woerle, H.J. Lack of Drug-Drug Interaction between Empagliflozin, a Sodium Glucose Cotransporter 2 Inhibitor, and Warfarin in Healthy Volunteers. *Diabetes, obesity & metabolism* **2013**, *15*, 316–323. https://doi.org/10.1111/dom.12028.
72. Macha, S.; Koenen, R.; Sennewald, R.; Schöne, K.; Hummel, N.; Riedmaier, S.; Woerle, H.J.; Salsali, A.; Broedl, U.C. Effect of Gemfibrozil, Rifampicin, or Probenecid on the Pharmacokinetics of the SGLT2 Inhibitor Empagliflozin in Healthy Volunteers. *Clinical therapeutics* **2014**, *36*, 280–290.e1. https://doi.org/10.1016/j.clinthera.2014.01.003.
73. Macha, S.; Mattheus, M.; Pinnetti, S.; Broedl, U.C.; Woerle, H.J. Pharmacokinetics of Empagliflozin and Pioglitazone After Coadministration in Healthy Volunteers. *Clinical therapeutics* **2015**, *37*, 1503–1516. https://doi.org/10.1016/j.clinthera.2015.05.002.
74. van der Aart-van der Beek, A.B.; Wessels, A.M.A.; Heerspink, H.J.L.; Touw, D.J. Simple, Fast and Robust LC-MS/MS Method for the Simultaneous Quantification of Canagliflozin, Dapagliflozin and Empagliflozin in Human Plasma and Urine. *Journal of chromatography. B, Analytical technologies in the biomedical and life sciences* **2020**, *1152*, 122257. https://doi.org/10.1016/j.jchromb.2020.122257.
75. Balaur, I.; Nickerson, D.P.; Welter, D.; Wodke, J.A.; Ancien, F.; Gebhardt, T.; Grouès, V.; Hermjakob, H.; König, M.; Radde, N.; et al. FAIRification of Computational Models in Biology, 2025. https://doi.org/10.1101/2025.03.21.644517.